Human Molecular Genetics, 2010, Vol. 19, No. 15 **2974–2986**
doi:10.1093/hmg/ddq202
Advance Access published on May 11, 2010

ALS-linked mutant SOD1 damages mitochondria by promoting conformational changes in Bcl-2

Steve Pedrini[1,†], Daniela Sau[1,†], Stefania Guareschi[1,2], Marina Bogush[1], Robert H. Brown Jr[3], Nicole Naniche[1], Azadeh Kia[1], Davide Trotti[1] and Piera Pasinelli[1,*]

[1]Frances and Joseph Weinberg Unit for ALS Research, Farber Institute for Neurosciences, Department of Neuroscience, Thomas Jefferson University, Philadelphia, PA 19107, USA, [2]Neurological Institute IRCCS 'C. Mondino', Pavia, Italy and [3]Department of Neurology, University of Massachusetts School of Medicine, Worcester, MA 01655, USA

Received March 3, 2010; Revised April 19, 2010; Accepted May 7, 2010

In mutant superoxide dismutase (SOD1)-linked amyotrophic lateral sclerosis (ALS), accumulation of misfolded mutant SOD1 in spinal cord mitochondria is thought to cause mitochondrial dysfunction. Whether mutant SOD1 is toxic *per se* or whether it damages the mitochondria through interactions with other mitochondrial proteins is not known. We previously identified Bcl-2 as an interacting partner of mutant SOD1 specifically in spinal cord, but not in liver, mitochondria of SOD1 mice and patients. We now show that mutant SOD1 toxicity relies on this interaction. Mutant SOD1 induces mitochondrial morphological changes and compromises mitochondrial membrane integrity leading to release of Cytochrome C only in the presence of Bcl-2. In cells, mouse and human spinal cord with SOD1 mutations, the binding to mutant SOD1 triggers a conformational change in Bcl-2 that results in the uncovering of its toxic BH3 domain and conversion of Bcl-2 into a toxic protein. Bcl-2 carrying a mutagenized, non-toxic BH3 domain fails to support mutant SOD1 mitochondrial toxicity. The identification of Bcl-2 as a specific target and active partner in mutant SOD1 mitochondrial toxicity suggests new therapeutic strategies to inhibit the formation of the toxic mutant SOD1/Bcl-2 complex and to prevent mitochondrial damage in ALS.

INTRODUCTION

Amyotrophic lateral sclerosis (ALS) is a neurodegenerative disease characterized by death of spinal and cranial motor neurons (1). Three percent of ALS arises from mutations in copper–zinc superoxide dismutase [SOD1 (2)] which acquires new toxic functions not fully defined (1). Although SOD1 is cytosolic, a portion (~1–2%) partitions in the mitochondria (3–8). Mitochondrial accumulation of misfolded mutant SOD1 (mutSOD1) has been proposed as one possible trigger of mutSOD1-mediated motor neuron death (9). Mitochondrial degeneration (10), vacuolization and swelling (11) are pathological features of both familial mutSOD1-linked human ALS cases and mutSOD1 mouse models. In SOD1-G93A mice mitochondrial degeneration precedes disease symptoms, culminating at disease onset (9,12). SOD1-G93A mice show dysfunctional mitochondria with reduced ATP production (13), oxidative phosphorylation (14,15) and calcium buffering capacity (16). Mitochondrial axonal transport is also impaired (17,18).

Mitochondrial mutSOD1 may directly damage these organelles by forming toxic aggregates (5). Nevertheless, it is not known if aggregated mutSOD1 is *per se* toxic to mitochondria or if, to cause toxicity, mutSOD1 engages in abnormal interactions with other mitochondrial proteins. We identified an aberrant interaction between mutSOD1 and Bcl-2 specific of spinal cord mitochondria (7), and now show that to damage the mitochondria, mutSOD1 relies on this interaction with Bcl-2.

*To whom correspondence should be addressed at: Frances and Joseph Weinberg Unit for ALS Research, Farber Institute for Neuroscience, JHN451, Department of Neuroscience, Thomas Jefferson University, 900 Walnut Street, Philadelphia, PA 19107, USA. Tel: +1 2159558394; Fax: +1 2155039128; Email: piera.pasinelli@jefferson.edu
†S.P. and D.S. contributed equally to this work.

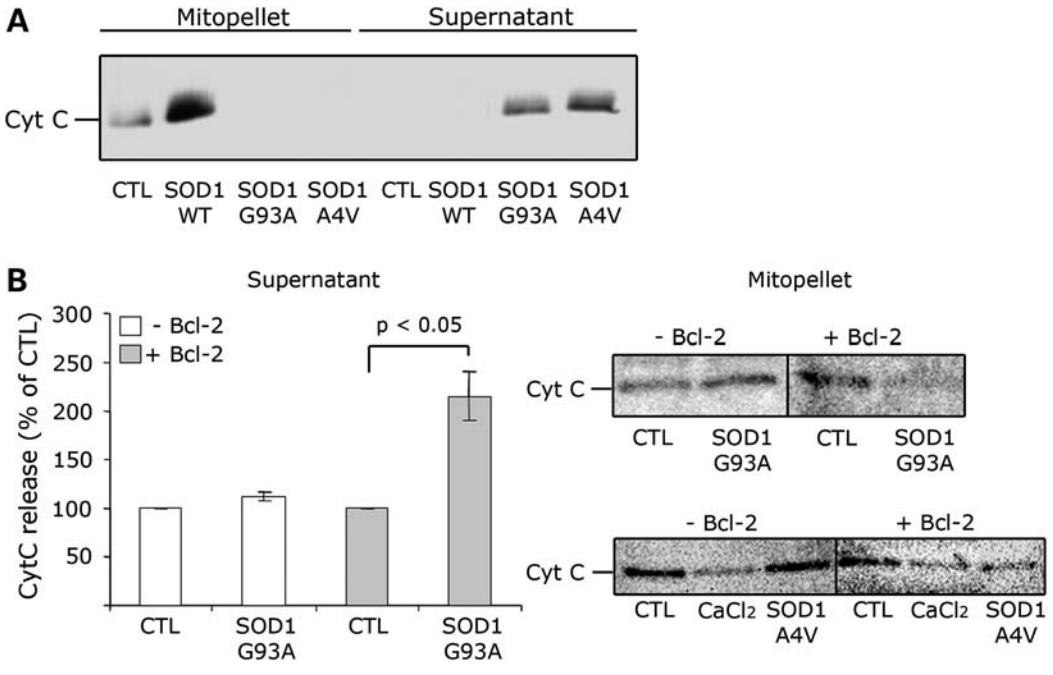

Figure 1. In isolated mitochondria, mutSOD1 induces Cytochrome C release only in the presence of Bcl-2. (**A**) Mitochondria isolated from mouse spinal cord were incubated with 1 mM of recombinant SOD1 (WT, G93A and A4V) for 30 min. Samples were then ultracentrifuged and the mitochondrial (mitopellet) and cytosolic (supernatant) fractions analyzed by WB with an anti-Cytochrome C antibody. Only mutSOD1 reduces Cytochrome C in the mitopellet and increases it in the supernatant fraction. (**B**) Bcl-2 negative or Bcl-2 positive mitochondria isolated from HEK293T cells were incubated with recombinant SOD1-G93A as above and Cytochrome C levels measured in supernatant by ELISA (left panel) and mitopellet by WB (right-upper panel). ELISA data are mean ± SEM of four independent experiments. Mitopellet shows a representative WB. Data were also confirmed with SOD1-A4V-treated mitochondria and analyzed by WB (right-lower panel). $CaCl_2$ was used as control for maximal loss of mitochondrial integrity.

Normally a pro-survival protein and a key factor in the regulation of mitochondrial membrane potential (19), Bcl-2 can reverse its functional phenotype and become a toxic protein (20). Bcl-2 contains four functional motifs called Bcl-2 homology (BH) domains (BH1–BH4) (21). The BH1 and BH2 domains are involved in pore formation; the BH3 and BH4 domains are the toxic and pro-survival domains, respectively (20). In normally functioning non-toxic Bcl-2, the BH1–BH3 domains form a hydrophobic pocket that buries the BH3 domain to prevent toxic activities. Conversion of Bcl-2 functional phenotype involves rearrangement of the quaternary structure through reorganization of the unstructured loop region (22,23) and exposure of toxic BH3 domain. These conformational changes are induced by binding with toxic proteins like Nur77 (23,24) or p53 (25) or toxic reagents like gossypol (26).

Here we show that mutSOD1 converts Bcl-2 into a toxic molecule, making it an active accomplice of its own toxicity. In isolated mitochondria and in cells, Bcl-2 becomes an essential target of mutSOD1 and undergoes a conformational modification, exposing the toxic BH3 domain. The mutSOD1-induced conformational change in Bcl-2 is also evident in ALS mice and patients with mutated SOD1. The ability of mutSOD1 to convert Bcl-2 into a toxic protein offers the opportunity to design drugs that by inhibiting the binding between mutSOD1 and Bcl-2 could restore or preserve Bcl-2 normal conformation and function, thereby maintaining the integrity of the mitochondria.

RESULTS

MutSOD1-mediated mitochondrial toxicity requires Bcl-2

Mitochondrial recruitment and accumulation of misfolded mutSOD1 have been suggested to play a significant role in the mitochondrial dysfunction observed in ALS (1,9,12). To determine whether mutSOD1 can directly damage the mitochondria, we incubated recombinant mutSOD1 (27), consisting of a mixture of monomeric and oligomeric forms, with purified mitochondria isolated from mouse spinal cord. We found that contrary to wild type (WT), mutSOD1 impaired the mitochondria as denoted by the release of Cytochrome C (Fig. 1A), indicating that at least *in vitro*, mutSOD1 directly damages the mitochondria. The challenge then is to identify the mechanism of this direct toxicity.

We previously identified by immunoprecipitation an aberrant and possibly harmful interaction between mutSOD1 and Bcl-2 in spinal cord mitochondria (7) and hypothesized that mutSOD1-mediated toxicity depends on this interaction. Although the nature of this interaction was recently disputed (28), the data presented in Supplementary Material, Fig. S1 confirm the genuine specificity of the SOD1/Bcl-2 association both in mouse spinal cord (Supplementary Material, Fig. S1A) and cultured cells (Fig. S1B). Control IgGs, corresponding to the precipitating antibodies, failed to aspecifically co-precipitate SOD1 and Bcl-2 in mouse spinal cord (Supplementary Material, Fig. S1A). Moreover, the anti-SOD1 antibody used in the immunoprecipitation did not

react, and therefore did not precipitate, with any aspecific band in ~25–30 kDa range in Bcl-2 lacking HEK293T cells (Supplementary Material, Fig. S1B), attesting the specificity of the SOD1/Bcl-2 co-immunoprecipitation and further validating our findings.

Thus, to determine whether mutSOD1 is intrinsically toxic or requires Bcl-2 to induce mitochondrial damage, we measured the release of Cytochrome C from mitochondria isolated from non-transfected HEK293T cells (Bcl-2 negative mitochondria) or from HEK293T cells transiently transfected with Bcl-2 (Bcl-2 positive mitochondria) and incubated with recombinant mutSOD1 (A4V or G93A) as above. As shown in Supplementary Material, Fig. S1C, the extensively characterized HEK293T cells lack detectable levels of Bcl-2 (24) and therefore represent a suitable tool to study the effect of mutSOD1 in the absence of Bcl-2. Cytochrome C released from mitochondria was analyzed by ELISA (Fig. 1B-supernatant), whereas the amount of Cytochrome C retained in the mitochondrial pellet was determined by western blot [WB (Fig. 1B-mitopellet)]. SOD1-G93A did not induce a Cytochrome C release in the medium in which the Bcl-2 negative mitochondria were suspended (Fig. 1B-supernatant). Accordingly, Bcl-2 negative mitochondria retained Cytochrome C when incubated with SOD1-G93A (Fig. 1B-mitopellet). When incubated with Bcl-2 positive mitochondria (derived from Bcl-2-transfected HEK293T cells), mutSOD1 induced a 2-fold increase in Cytochorme C released into the supernatant ($P < 0.05$, Fig. 1B-supernatant). Similar results were obtained with mutSOD1-A4V. Only in Bcl-2 positive mitochondria, incubation with SOD1-A4V led to a 40% decrease of Cytochrome C in the mitopellet (Fig. 1B-mitopellet). Contrary to mutSOD1s, SOD1-WT did not induce a release of Cytochrome C from either Bcl-2 negative or positive mitochondria (data not shown).

The requirement of Bcl-2 for mutSOD1-mediated mitochondrial damage was confirmed in cells *in situ*. HEK293T cells were either transfected with eGFP-tagged SOD1s (WT and G93A) as control, or co-transfected with eGFP-tagged SOD1s and Bcl-2. Transfection with Bcl-2 alone or co-transfection with the eGFP empty vector was also used as additional control. Twenty-four hours after transfection, mitochondrial integrity was determined by immunofluorescence using an anti-Cytochrome C antibody and confocal microscopy analysis. Transfection of either Bcl-2 or SOD1 (WT and G93A) alone did not damage the mitochondria. This is illustrated in single transfected HEK293T cells by the punctate immunofluorescence indicative of Cytochrome C retention into intact mitochondria (Fig. 2A). In contrast, in 85% of HEK293T cells co-expressing Bcl-2 and mutant, but not SOD1-WT, there was diffuse Cytochrome C immunofluorescence, indicating that release of Cytochrome C from damaged mitochondria had occurred (Fig. 2A and B). Release of Cytochrome C was also detected in mitochondrial pellets by WB (Fig. 2C). As determined by densitometric analysis, Cytochorme C decreased by 35% only in the mitochondrial pellet derived from cells expressing both Bcl-2 and mutSOD1 (Fig. 2C-right panel). There was no significant loss of mitochondrial Cytochorme C in cells expressing either Bcl-2 or mutSOD1 alone. Together with the evidence collected in isolated mitochondria, these results indicate that mutSOD1-mediated loss of mitochondrial integrity relies on the presence of Bcl-2, underscoring the importance of the mutSOD1/Bcl-2 complex in the regulation of mitochondrial viability.

MutSOD1 and Bcl-2 induce morphological alterations in mitochondria

To investigate if the release of Cytochrome C mediated by mutSOD1 and Bcl-2 was accompanied by structural alterations of the mitochondria, we analyzed mitochondrial morphology by transmission electron microscopy in HEK293T cells co-transfected with mutSOD1 and Bcl-2 or control cells co-transfected with mutSOD1 + control plasmid or Bcl-2 + SOD1-WT. Figure 3 shows results representative of four independent experiments. For each experiment, 8–10 fields of vision were randomly photographed under the transmission electron microscope. A comparison between the experimental groups was then made by scoring the percentage of damaged mitochondria/field. For each experimental group, transfection efficiency was determined by WB analysis of SOD1-eGFP and Bcl-2, respectively (Fig. 3B). One hundred percent of non-transfected, control HEK293T cells had elongated mitochondria with intact internal structure and cristae organization (Fig. 3A, panel A). Single transfection of SOD1 (WT or mutant), or Bcl-2 did not induce any morphological change in mitochondria [95% of mitochondria retained intact membrane and cristae (Fig. 3A, panels B, C and D)]. Similarly, when co-transfected with SOD1-WT, Bcl-2 did not alter the mitochondria morphology [97% of intact mitochondria (Fig. 3A, panel E)]. HEK293T cells co-expressing mutSOD1 and Bcl-2 were instead characterized by a vast majority (80%) of rounded, swollen mitochondria with deranged cristae and extensive vacuolization (Fig. 3A, panel F). This aberrant mitochondrial morphology in response to co-expression of mutSOD1 and Bcl-2 was not the aspecific consequence of protein overload due to different degrees of transfection in the various experimental groups, as WB analysis of Bcl-2 and SOD1 (WT and mutant) showed comparable expression levels among different samples (Fig. 3B).

MutSOD1 damages the mitochondria by triggering a conformational change in Bcl-2 which exposes the toxic BH3 domain

Upon binding to toxic proteins like Nur77 (24) and p53 (25), Bcl-2 gains a novel toxic function, triggered by a structural modification that exposes the toxic BH3 domain. To study whether binding to mutSOD1 altered Bcl-2 conformation exposing the toxic BH3 domain, we employed immunoprecipitation and flow cytometry analysis using anti-Bcl-2 (α-Bcl-2) conformation-specific antibodies (24). We used the α-Bcl-2/pocket, which recognizes conformationally normal Bcl-2 in which the pocket region masks the toxic BH3 domain, the α-Bcl-2/BH3 domain, which binds only to conformationally altered Bcl-2 in which the toxic BH3 domain is exposed and the α-Bcl-2 antibody, which binds to the loop domain and is accessible in both BH3-masked and BH3-exposed Bcl-2 proteins (see Supplementary Material, Fig. S2A).

We studied the effect of mutSOD1 on Bcl-2 conformation in neuronal SH-SY5Y cells (Fig. 4A) that endogenously express Bcl-2 and were therefore transfected with SOD1

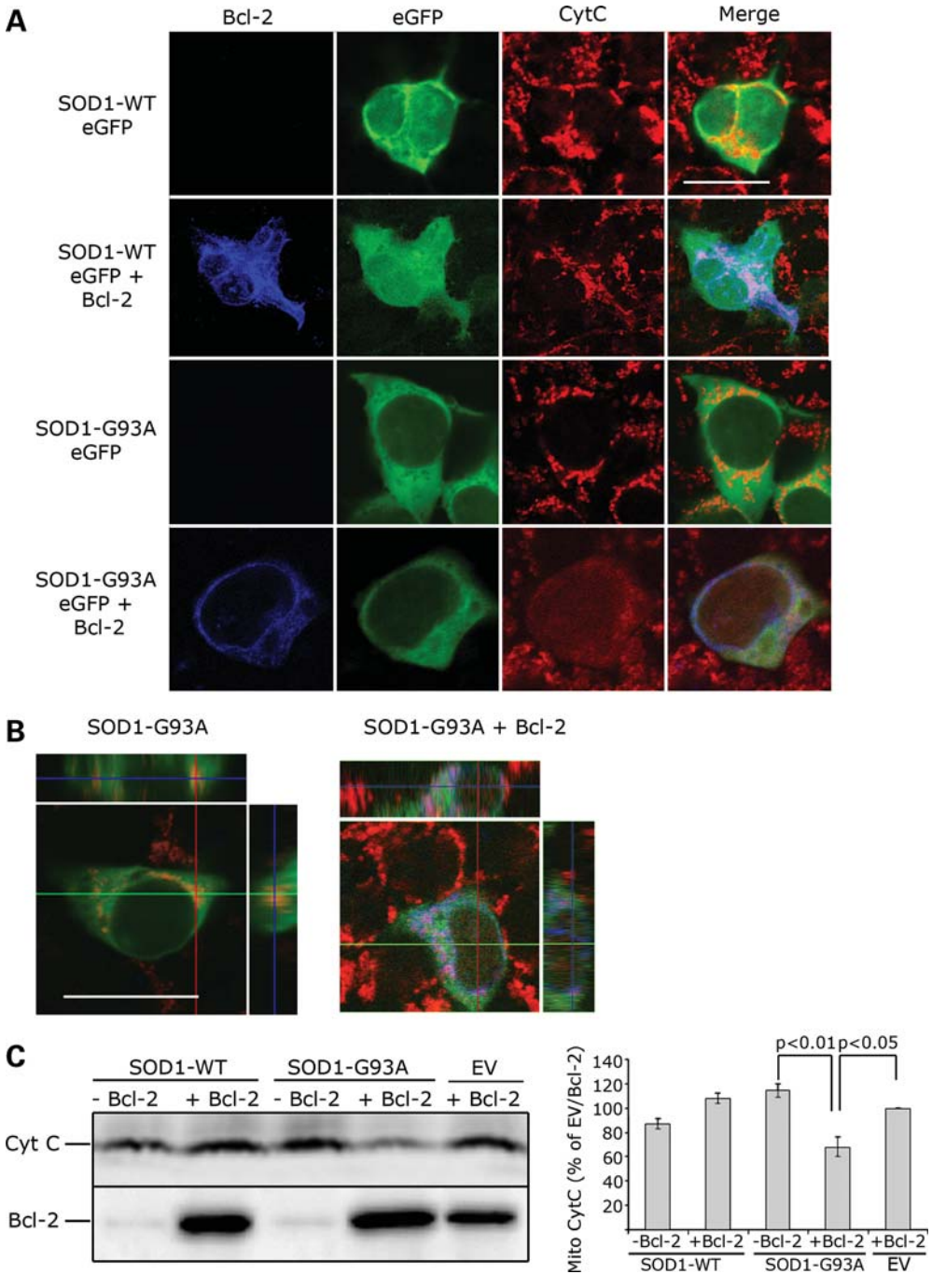

Figure 2. Co-expression of Bcl-2 and mutant, but not SOD1-WT, damages the mitochondria. (**A**) Mitochondrial integrity was assessed by confocal microscopy analysis of HEK293T cells transfected with SOD1-eGFP (WT or G93A) in the presence or absence of Bcl-2 and stained with anti-Cytochrome C antibody. For each experiment ($n = 4$), 10 fields of vision were randomly photographed and the percentage of cells co-expressing mutSOD1 (green) and Bcl-2 (blue) with damaged mitochondria was counted. Approximately 85% of cells show damaged mitochondria with diffuse Cytochrome C staining. In cells expressing SOD1-G93A alone, Cytochrome C staining is punctuate, indicative of structurally intact mitochondria. In 98% of SOD1-WT-positive cells, either in the presence or absence of Bcl-2, staining of Cytochrome C is punctuate (intact mitochondria). Scale bar 20 μm. (**B**) z-stack orthogonal views are shown to confirm mitochondrial integrity and Cytochrome C staining within the cell. Scale bar 20 μm. (**C**) Representative WB of mitochondrial Cytochrome C. Mitochondria were isolated from HEK293T cells and the total amount of Cytochrome C retained and/or released from the mitopellet assessed by WB. MutSOD1 and Bcl-2 induce a decrease of Cytochrome C in mitochondria, whereas expression of either molecule alone does not (top lane). Efficiency of transfection was evaluated by probing for Bcl-2 (bottom lane). The histogram shows intensity of Cytochrome C staining in mitopellet measured by densitometric analysis using the Biorad Chemidoc Quantity One software. Data are mean (mean + SEM) of three independent experiments. Student's *t*-test shows statistically significant differences between experimental groups. EV = empty vector.

proteins only (WT, G37R or G93A). When compared with cells transfected with SOD1-WT, transfection of mutSOD1 proteins decreased the exposure of the pocket region and therefore the amount of Bcl-2 immunoprecipitated by the α-Bcl-2/pocket antibody, and led to an increase in Bcl-2 immunoprecipitated by the α-Bcl-2/BH3 antibody (Fig. 4A, left panel), indicating that in the presence of mutSOD1, Bcl-2 underwent a structural change allowing exposure of the normally buried toxic

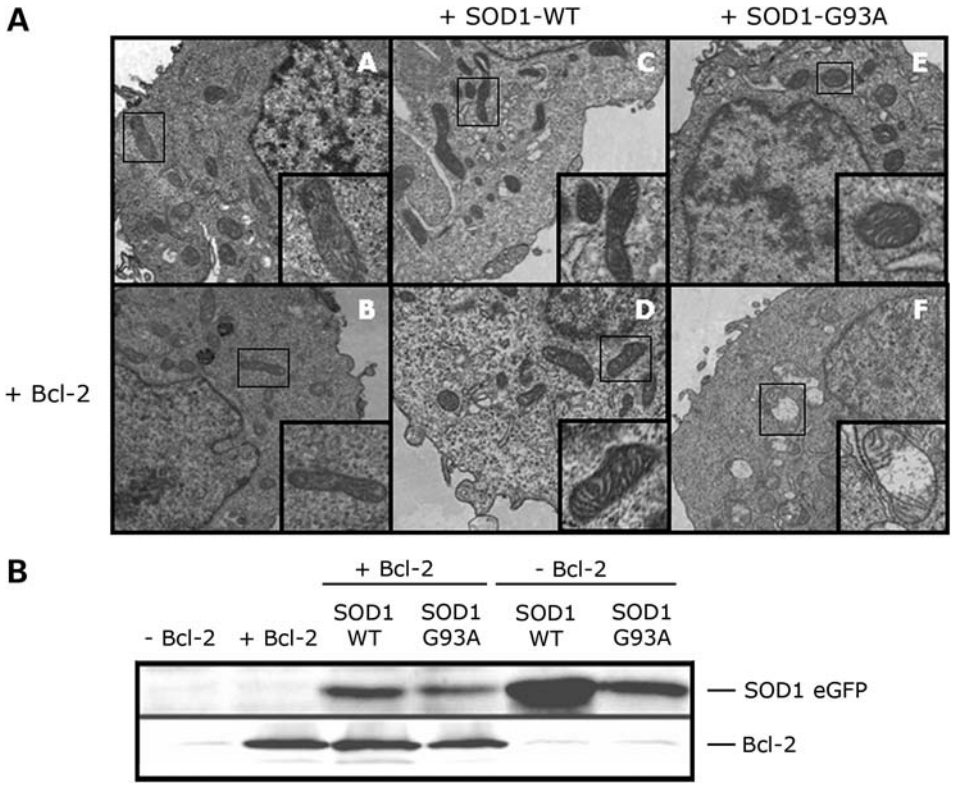

Figure 3. Co-expression of SOD1-G93A and Bcl-2 induces mitochondrial structural damage. (**A**) Electron microscopy analysis of mitochondrial structure in HEK293T transfected with SOD1-WT (panels C and D), SOD1-G93A (panels E and F) without (upper panels A, C and E) or with (lower panels B, D and F) Bcl-2. Cells transfected with SOD1-G93A alone show structurally normal mitochondria (panel E), whereas co-expression of Bcl-2 and SOD1-G93A causes morphological changes as shown by extensive internal vacuolization and cristae disorganization (panel F). Images are representative of four experiments. (**B**) Transfection efficiency and expression levels of SOD1-eGFP and Bcl-2 among different experimental groups were assessed by WB with an anti-eGFP and Bcl-2 antibody, respectively.

BH3 domain and loss of usually 'protective' conformation. The ratio BH3/pocket increased in the presence of mutSOD1, whereas it remained virtually unchanged in cells transfected with SOD1-WT (Fig. 4A, right panel). The fact that two different mutSOD1 proteins (G37R and G93A) induced a similar conformational change in Bcl-2 indicates that the exposure of the toxic BH3 domain in the mutSOD1/Bcl-2 complex is a shared feature among ALS-linked SOD1 mutants. We confirmed this by flow cytometry (Supplementary Material, Fig. S2B) in SH-SY5Y cells transiently transfected with eGFP-tagged SOD1-G37R and G93A. In agreement with the immunoprecipitation experiments, Bcl-2/BH3 immunofluorescence was absent in non-transfected cells (Supplementary Material, Fig. S2B) and negligible in eGFP expressing cells used as mock-transfected control (not shown). A significant Bcl-2/BH3 immunofluorescence was instead detected in both SOD1-G37R and G93A transfected cells (Supplementary Material, Fig. S2B), confirming the conformational change in Bcl-2 triggered by mutSOD1.

In mutSOD1 ALS mice and patients Bcl-2 undergoes a conformational change that exposes the toxic BH3 domain

We next studied whether exposure of the toxic BH3 domain occurs *in vivo* and extended our analysis to the well-characterized SOD1-G93A mouse model of ALS. Immunoprecipitation and WB analysis of spinal cord homogenates prepared from 130-day-old SOD1-G93A mice (end-stage), showed a significant exposure of the toxic BH3 domain compared with spinal cord homogenates prepared from age-matched SOD1-WT over-expresser mice (Fig. 4B). Exposure of the toxic BH3 domain was paralleled by a decrease in binding affinity for the Bcl-2/pocket domain reflecting a loss of the normal protective function of Bcl-2. This Bcl-2 structural conformational change increased as disease progressed in the SOD1-G93A mice (Fig. 4C), appearing in 30-day-old pre-symptomatic mice and peaking at disease onset (85 days). Densitometric analysis of the immunoprecipitated Bcl-2 (Fig. 4C, right panel) showed that the ratio BH3/pocket reverses during progression of the disease, with the minimum BH3 exposure at 30 days (early pre-symptomatic stage) and the highest at disease onset (85 days). This gradual appearance (Fig. 4C, right panel) of the toxic BH3 domain strongly suggests the disease specificity of the conformational change in Bcl-2.

A similar conformational modification in Bcl-2 was seen in a spinal cord homogenate prepared from an SOD1-A4V ALS patient (Fig. 4D).

Co-expression of mutSOD1 and BH3-inactive Bcl-2 no longer damages mitochondria and does not compromise cell viability

To confirm that exposure of the toxic BH3 domain is a relevant mechanism in mutSOD1-induced mitochondrial damage, we

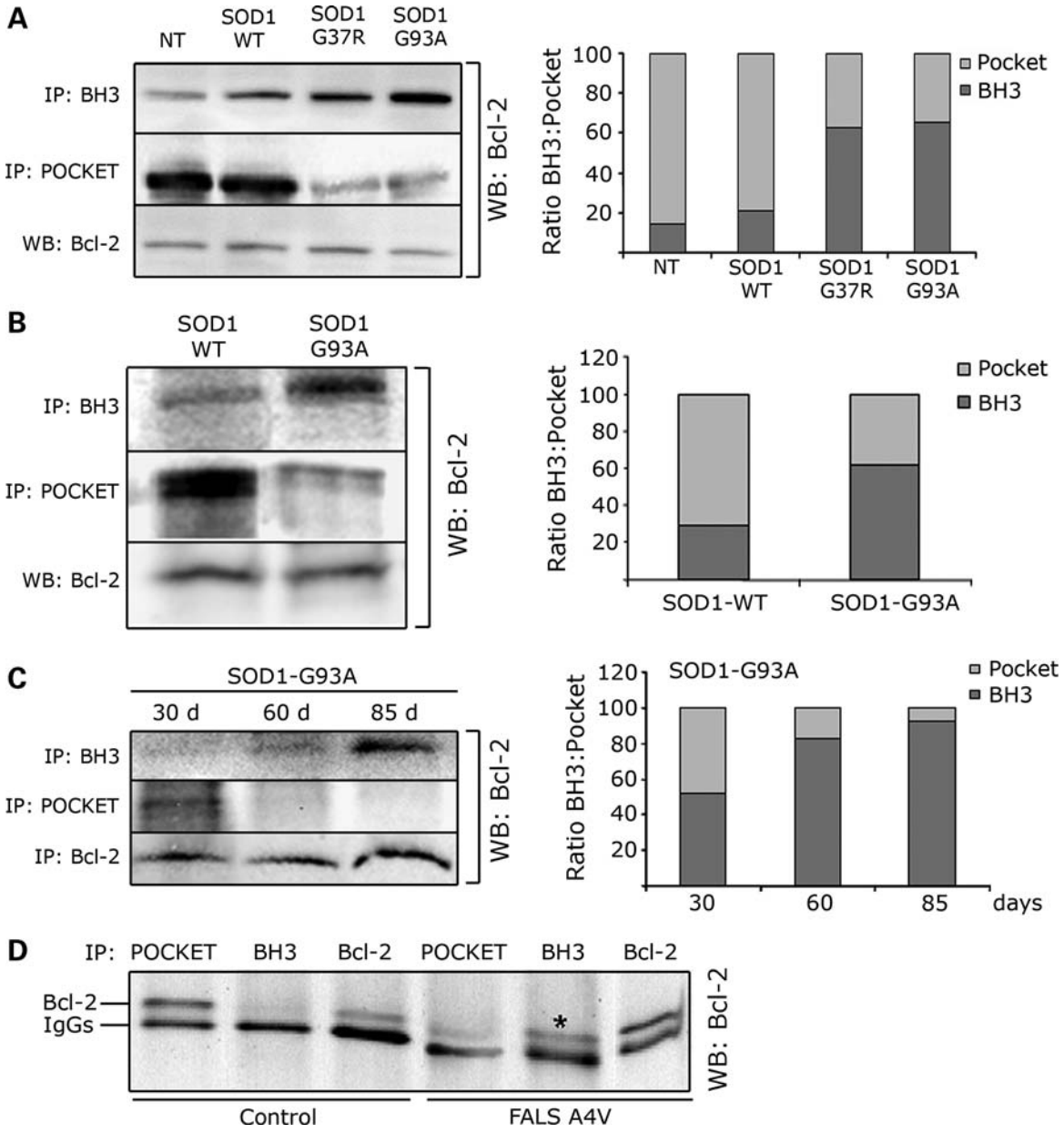

Figure 4. MutSOD1s induce a conformational change in Bcl-2 leading to exposure of the toxic BH3 domain in cells, mouse and human spinal cords. (**A**) SH-SY5Y cells, which express endogenous Bcl-2, were transfected with SOD1 (WT, G37R or G93A) and Bcl-2 conformation assessed by immunoprecipitation with the α-Bcl-2/BH3 and α-Bcl-2/pocket antibody, respectively. Immunoprecipitated proteins were analyzed by WB with anti-Bcl-2 antibody against the N-terminal domain (left panel). Total amount of Bcl-2 was assessed by WB (left panel, bottom lane). In the presence of mutSOD1s (G37R and G93A), there is an increased exposure of the toxic BH3 domain paralleled by a decrease in the pocket region. The plot in the right panel shows the ratio BH3/pocket as analyzed by densitometric analysis of the immunoprecipitated Bcl-2 with the Quantity One software. (**B**) The α-Bcl-2/BH3 and α-Bcl-2/pocket antibodies were used to immunoprecipitate Bcl-2 from spinal cord homogenates of 130-day-old transgenic mice expressing either SOD1-WT or SOD1-G93A. In SOD1-G93A mice there is an increased exposure of the toxic BH3 domain of Bcl-2 compared with age-matched transgenic SOD1-WT mice, and this is paralleled by a decreased exposure of the pocket. (**C**) Conformational changes in Bcl-2 were then assessed over time in the SOD1-G93A mice. Exposure of the toxic BH3 domain appears prior to and peaks at disease onset (left panel). Densitometry analysis of the ratio BH3/pocket is shown in the plot on the right. (**D**) Immunoprecipitation of post-mortem human SOD1-A4V spinal cord shows increased exposure of the BH3 domain (shown as *) paralleled by a decreased exposure of the pocket region in human ALS.

generated a Bcl-2 in which the BH3 domain has been inactivated by mutating its core sequence ($Gly^{101}-Asp^{102}-Asp^{103} \rightarrow Ala^{101}-Ala^{102}-Ala^{103}$). This mutated Bcl-2(AAA) has been previously described to lose its ability to induce cellular toxicity and Cytochrome C release (29).

Whereas HEK293T cells co-expressing mutSOD1 and BH3-active Bcl-2 showed diffuse pattern of Cytochrome C staining indicative of damaged mitochondria (Fig. 2), HEK293T cells co-transfected with mutSOD1 and Bcl-2/BH3-inactive displayed Cytochrome C punctate staining

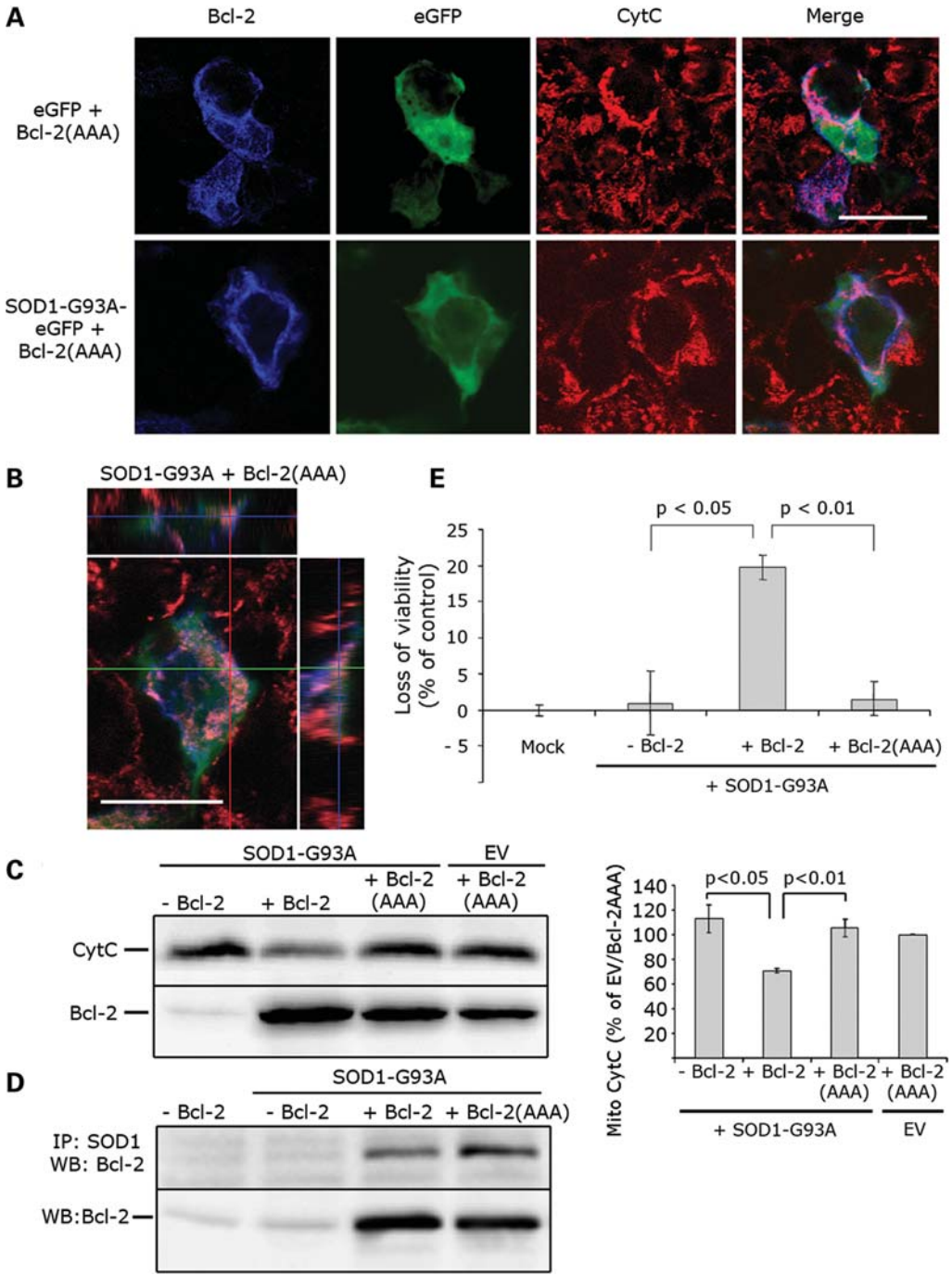

Figure 5. BH3-inactive Bcl-2 abolishes mutSOD1 mitochondrial toxicity. (**A**) Representative confocal images. HEK293T cells were transfected with SOD1-G93A eGFP in the presence or absence of Bcl-2(AAA) for 24 h and mitochondrial integrity assessed by staining with the anti-Cytochrome C antibody. When co-transfected with Bcl-2(AAA), SOD1-G93A loses its toxicity on mitochondria and does not trigger a release of Cytochrome C. Scale bar 20 μm. (**B**) Mitochondrial integrity was also assessed with z-stack orthogonal views. Scale bar 20 μm. (**C**) Cytochrome C release from damaged mitochondria was confirmed biochemically. Mitochondria were isolated from HEK293T cells co-transfected with SOD1-G93A and Bcl-2(AAA) and the amount of mitochondrial Cytochrome C measured in the mitopellet by WB. Cytochrome C is retained in the mitochondria in cells with SOD1-G93A and Bcl-2(AAA) (top lane), indicating only little or no damage to the mitochondria. Efficiency of transfection was evaluated by probing for Bcl-2 (bottom lane). The histogram in the right panel shows the results of densitometric analysis of mitochondrial Cytochrome C staining. Data are mean (mean + SEM) of four experiments. Student's *t*-test shows statistically significant differences between experimental groups. (**D**) Bcl-2(AAA) retains its binding properties with SOD1-G93A. HEK293T cells were co-transfected with SOD1-G93A and either Bcl-2 or Bcl-2(AAA), lysed and immunoprecipitated with the anti-SOD1 antibody. Binding to Bcl-2 was determined by WB (top lane). Efficiency of transfection was evaluated by probing for Bcl-2 (bottom lane). (**E**) HEK293T cells were transfected with an empty vector (Mock), SOD1-G93A alone or in combination with Bcl-2 or Bcl-2(AAA). SOD1-G93A induces a loss of viability in the presence of BH3-active Bcl-2, but not in cells in which the BH3 domain is inactive. Student's *t*-test was performed to determine differences between groups.

characteristic of healthy mitochondria (Fig. 5A and B). WB analysis of Cytochrome C in the mitochondrial pellet derived from HEK293T cells showed reduced mitochondrial Cytochrome C only in cells co-transfected with mutSOD1 and BH3-active Bcl-2. In cells co-transfected with mutSOD1 and Bcl-2(AAA), Cytochrome C levels were unaffected (Fig. 5C). The absence of mitochondrial damage in the presence of Bcl-2(AAA) is not due to lack of binding between mutSOD1 and Bcl-2(AAA). Co-immunoprecipitation experiments (Fig. 5D) in HEK293T cells confirmed that Bcl-2(AAA) is still able to bind and co-precipitate with mutSOD1 (Fig. 5D).

We next studied whether inactivation of the BH3 domain is also able to block the downstream effects of the toxic mutSOD1/Bcl-2 complex on the viability of HEK293T cells. We used the CellTiter-Glo Luminescent Cell Viability Assay which measures the number of metabolically active cells/well. As expected, co-expression of mutSOD1 and BH3-active Bcl-2 induced a significant loss of cell viability (~25%) whereas co-expression of mutSOD1 and Bcl-2(AAA) did not. These data confirm that mutSOD1-mediated toxicity proceeds through exposure of the toxic BH3 domain.

Toxicity of the mutSOD1/Bcl-2 complex is organelle-specific

To determine whether the toxicity caused by the mutSOD1/Bcl-2 complex required specific mitochondrial localization of Bcl-2 within the cell, we transfected HEK293T cells with mutSOD1 and Bcl-2 lacking its *trans*-membrane domain (Bcl-2/ΔTM) and therefore unable to anchor itself to the outer mitochondrial membrane. Damage of the outer mitochondrial membrane required simultaneous mitochondrial localization of mutSOD1 and Bcl-2 because leakage of Cytochrome C did not occur in cells co-transfected with mutSOD1 and Bcl-2/ΔTM (Fig. 6A). Although Bcl-2/ΔTM was present in the cells and expressed in equal amounts compared with Bcl-2 WT (Fig. 6A), mutSOD1 lost its toxic properties on the mitochondria. Interestingly, mutSOD1 did not impair cell viability when co-expressed with Bcl-2/ΔTM (Fig. 6B) strongly arguing in favor of an organelle-specific effect of the mutSOD1/Bcl-2 complex. Further, in H4 cells that appear to express exclusively nuclear Bcl-2, mutSOD1 lost its mitochondrial toxic effect (Supplementary Material, Fig. S3), indicating that toxicity mediated by the mutSOD1/Bcl-2 complex requires anchoring of Bcl-2 to the mitochondrial outer membrane.

DISCUSSION

We dissected the mechanism(s) by which mutSOD1 damages the mitochondria. We focused on the mutSOD1/Bcl-2 interaction because in mutSOD1 ALS mice and patients, we previously identified this aberrant protein complex occurring in spinal cord but not liver mitochondria (7), a pattern that correlates with the tissue specificity of the disease. We therefore hypothesized that to damage the mitochondria mutSOD1 relies on mitochondrial Bcl-2. The results presented here support this hypothesis. We show that mutSOD1 targets mitochondrial Bcl-2 and converts it into a toxic protein that actively participates in mutSOD1-mediated mitochondrial toxicity.

Mitochondria degeneration is recognized as a component of mutSOD1 toxicity in ALS. The observation that misfolded mutSOD1 accumulates in spinal cord mitochondria (5) and that only mitochondria with mutSOD1 inclusions degenerate (30) suggests that these organelles are a primary target of mutSOD1-mediated toxicity. Whether accumulation of misfolded mutSOD1 at the mitochondria is a secondary event of disease progression, or whether mitochondrial mutSOD1 actively damages the mitochondria is not known. Here we show that *in vitro*, addition of purified mutant, but not SOD1-WT, to mitochondria isolated either from cultured cells or spinal cord tissues damages the mitochondria ultimately leading to Cytochrome C release. These results provide a cause-effect link between mutSOD1 and loss of integrity of the mitochondrial membranes, strongly suggesting that mutSOD1 actively damages the mitochondria.

How does mitochondrial mutSOD1 damage the mitochondria? Does it act alone or does it require a partner(s) in crime? Formation of vacuoles in the outer mitochondrial membrane (31) or protein aggregates that clog or disrupt the TOM complex (5), could either be potential mechanisms by which mutSOD1 alone impairs the mitochondria. Alternatively, mutSOD1 could interact with other vital mitochondrial proteins like Bcl-2 (7) and/or the recently identified mitoKARS (32). Here we show that in the absence of Bcl-2, mutSOD1 loses its toxic effect on isolated mitochondria, indicating that rather than acting alone, mutSOD1 requires Bcl-2 to damage the mitochondria. Thus, Bcl-2 is not simply a hostage protein, but it becomes an active accomplice of mutSOD1-mediated mitochondrial toxicity.

Bcl-2 is an essential regulator of mitochondria viability (20); it forms pore-like channels spanning one or both mitochondrial membranes whose activity is to offset mitochondrial ion imbalances induced by toxic stimuli or altered calcium uptake, restoring the mitochondrial membrane potential ($\Delta\psi$) to normal levels (33). Bcl-2 also directly binds and inhibits the toxic function of pro-death proteins like Bax and BaK (34), and prevents swelling of the mitochondrial matrix and uncontrolled production of reactive oxygen species (20,35). Bcl-2 can also lose these protective properties and reverse its phenotype into a lethal protein by undergoing a conformational change which exposes its toxic BH3 domain (22,24,29). Using conformation-specific Bcl-2 antibodies, we demonstrated that when bound to mutSOD1, Bcl-2 changes conformation and exposes its otherwise hidden BH3 domain, as reported when Bcl-2 interacts with toxic molecules like Nur77 and p53 (22). Through exposure of the toxic BH3 domain, Bcl-2 intensifies the mitochondrial damage caused by mutSOD1. When mutSOD1 binds to Bcl-2(AAA), a mutated form of Bcl-2 with an inactive BH3 domain, the mitochondrial membrane remains intact, and there is no leakage of Cytochrome C nor loss of cell viability. Thus, mutSOD1 converts Bcl-2 into a partner in crime which, most likely, targets surrounding mitochondrial proteins or other pro-survival members of the Bcl-2 proteins antagonizing and/or inhibiting their function. Studies are underway to examine these hypotheses.

We showed that SOD1-WT binds to the N-terminal portion of Bcl-2 between the BH4 and the loop domain (7). Although we used multiple Bcl-2 deletion mutants covering the entire Bcl-2 sequence, including the ΔBH4/loop mutant which

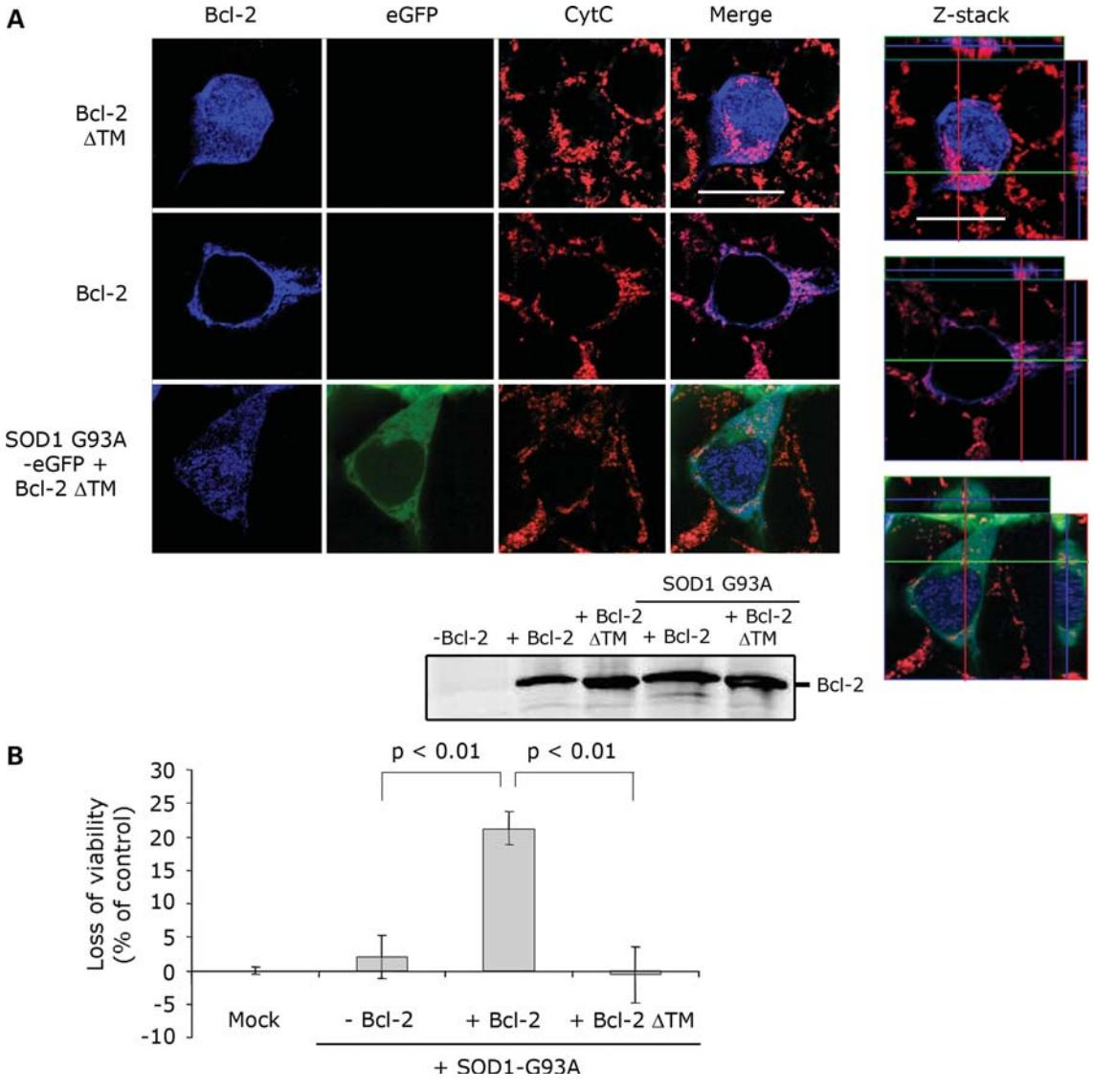

Figure 6. Anchoring of Bcl-2 to mitochondria is necessary for mutSOD1-induced toxicity. (**A**) HEK293T cells were co-transfected with SOD1-G93A and either Bcl-2 or Bcl-2 lacking the transmembrane domain (Bcl-2 ΔTM). When co-transfected with Bcl-2 ΔTM, which does not localize in mitochondria (diffuse blue staining), SOD1-G93A does no longer induce release of Cytochrome C. Efficiency of the transfection was evaluated by WB probing for Bcl-2. The integrity of mitochondria was also assessed by confocal analysis with *z*-stack orthogonal views (right). (**B**). HEK293T cells were transfected with empty vector (Mock), SOD1-G93A alone or in combination with Bcl-2 or Bcl-2 ΔTM. SOD1-G93A induces a loss of viability in the presence of Bcl-2, but not in Bcl-2 ΔTM-positive cells. Student's *t*-test shows statistically significant differences between experimental groups.

abolishes the binding with SOD1-WT, we failed to identify specific domains in Bcl-2 responsible for binding with mutSOD1. None of the Bcl-2 deletion mutants tested abolishes this binding, suggesting that mutSOD1 binding to Bcl-2 is conformation-specific and likely occurs on multiple distinct domains throughout the quaternary structure of Bcl-2. The unstructured loop domain of Bcl-2 links the BH4 to the BH3 domain and maintains the correct (pro-survival) conformation of Bcl-2 (23). Like other natively unstructured loops of the same class, the Bcl-2 loop domain adapts its structure upon different stimuli. When it is cleaved by caspases at position 34 (29,36) or when it is phosphorylated by stress-activated kinases (37), the loop domain rearranges Bcl-2 structure, inducing a conformational change. Binding of Nur77 and p53 at or near the loop domain induces a rearrangement of the hydrophobic cleft of Bcl-2, masking the pocket region and unmasking the toxic BH3 domain (24). Thus, if like WT, mutSOD1 binds at the interface with the loop domain but, unlike WT, engages Bcl-2 in a conformational aberrant binding which entraps multiple portions of the loop region, we suggest that mutSOD1 changes Bcl-2 conformation by acting on the loop domain, rearranging the hydrophobic cleft. Regardless, binding to Bcl-2 occurs only after mutSOD1 docking to the mitochondria. This is consonant with the lack of evidence for mutSOD1 localization in the nucleus or binding to nuclear Bcl-2 when mutSOD1 is expressed in H4 cells (Supplementary Material, Fig. S3), and with the evidence that mitochondria localization of Bcl-2 is required for

mutSOD1 to damage mitochondria (Fig. 6). In H4 cells in which Bcl-2 displays exclusive nuclear localization and in HEK293T cells transfected with Bcl-2/ΔTM, the mitochondria are unaffected by the presence of mutSOD1 and cells expressing mutSOD1 are viable and metabolically active. This suggests that toxicity of the mutSOD1/Bcl-2 complex is organelle-specific and also that docking of mutSOD1 to the mitochondria is independent of Bcl-2. Even in the absence of mitochondrial Bcl-2, a small portion of mutSOD1 resides in the mitochondria (Fig. 6), implying that mutSOD1 mitochondrial localization occurs independently of Bcl-2, perhaps through binding to other mitochondrial proteins.

Two observations underscore the tissue-specific pathogenic role of the mitochondrial mutSOD1/Bcl-2 complex. First, in ALS mice and patients this complex is specifically found in spinal cord but not liver mitochondria (7), in line with the tissue specificity of the disease. Second, in mutSOD1-G93A mice, the gradual conformational change in mitochondrial Bcl-2 correlates with disease progression in the spinal cord. We do not know whether this disease-related conformational change in Bcl-2 is motor neuron-specific or whether, within the spinal cord, it equally occurs in glia and neurons. The results presented in Fig. 4B and C, where the majority of spinal cord Bcl-2 gets converted into the toxic form in mutSOD1-G93A mice, suggest that this conversion occurs in virtually all cells and not only in the motor neurons as predicted by the non-cell autonomous nature of ALS. We do not know whether, although occurring in all cell types, formation of the mutSOD1/Bcl-2 complex is toxic only to the most vulnerable motor neurons or it equally damages other cells.

The conformational and phenotypic change in Bcl-2 induced by mutSOD1 may result in multiple harmful effects that ultimately weaken the mitochondria. The newly exposed BH3 domain may bind glutathione (GSH), inhibiting its antioxidant properties (38). Alternatively, in contrast to normally structured Bcl-2 which forms low conductance channels to maintain physiological mitochondrial $\Delta\psi$ (33,39), conformationally altered Bcl-2 may change its channel activity and dysregulate mitochondria bioenergetics ultimately causing Cytochrome C release. Compared with age-matched WT mice, pre-symptomatic SOD1-G93A and SOD1-G85R mice show an increased mitochondrial calcium-dependent $\Delta\psi$ depolarization which could result in reduced ATP synthesis at the synaptic terminals (40). Finally, binding to mutSOD1 may disrupt Bcl-2 binding to death-inducing proteins. In its normal conformation, the BH4 domain interacts with pro-death members of the Bcl-2 family and inhibits their toxic function (41). Following the conformational change induced by mutSOD1, the BH4 domain could become unavailable for binding, failing to antagonize pro-apoptotic proteins.

We favor the hypothesis that focuses on a direct toxic function of Bcl-2 on the mitochondria rather than on its potential to lose anti-apoptotic functions. This is because: (a) as disease progresses mitochondrial abnormalities precede motor neuron apoptotic death (1); (b) a recent report dissociated motor neuron dysfunction from apoptosis in ALS (28); (c) in neurons, after their conversion into toxic molecules, Bcl-2-like proteins induce mitochondrial alterations and decrease in synaptic function (42) independently from apoptotic mechanisms.

Since mitochondria regulate neuronal apoptosis and because activation of apoptotic pathways has been observed in ALS mice (1,43), the mitochondrial mutSOD1/Bcl-2 complex described in our previous work could have been interpreted as the mechanism by which mitochondrial mutSOD1 causes motor neuron apoptosis. However, the significance of apoptosis in ALS, and with that the significance of the pro-apoptotic function of the mutSOD1/Bcl-2 complex, has recently been challenged by the observation that ALS mice lacking the pro-apoptotic protein Bax develop motor neuron disease and mitochondrial abnormalities even in the absence of cell death (28). The findings presented here support rather than contradict this notion and may contribute to explain the paradoxical series of observations that argue against apoptotic cell death in ALS even though loss of motor neurons is accompanied by release of apoptogenic factors from the mitochondria and caspase activation (44–46). Our data suggest that, under stressful circumstances set in motion by mitochondrial mutSOD1, the normally pro-surviving Bcl-2 protein changes its phenotype, becomes toxic and destabilizes mitochondrial homeostasis through a mechanism independent of the classical cell death pathway. Consistent with this, gossypol (a polyphenolic compound shown to interact with Bcl-2) induces Bax/Bak independent Cytochrome C release and loss of $\Delta\psi$ by triggering a conformational change in Bcl-2 that exposes the toxic BH3 domain in $Bak^{-/-}/Bax^{-/-}$ cells (26). Similarly, in $Bax^{-/-}$SOD1-G93A mice (28), which lack developmental apoptosis but express Bcl-2, the mutSOD1/Bcl-2 complex may gain a new toxic function that triggers motor neuron dysfunction by directly damaging the mitochondria, ultimately impairing synaptic transmission at the neuromuscular junction.

Our work shows that mutSOD1 induces a gradual change in Bcl-2 conformation and function over time in the ALS mice. This result may also explain why over-expression of Bcl-2 in these mice only slightly delays disease onset without affecting disease duration (47). On the basis of our findings, one would expect that adding extra Bcl-2 in its normally protective conformation to the ALS mice would buy extra time and marginally delay disease onset. However, once the extra Bcl-2 is bound to mutSOD1, it no longer protects the motor neurons and instead becomes a toxic liability. Thus, our data suggest an alternative therapeutic strategy that targets the toxic binding between mutSOD1 and Bcl-2 instead of using Bcl-2 as a rescuing agent. BH3 and Bcl-2 like peptides are routinely used in cancer therapy (20); our data suggest that a similar therapeutic approach with peptides designed to compete or displace Bcl-2 from binding mutSOD1, can be tested in ALS mice and turned to our advantage to delay mitochondrial dysfunction in mutSOD1-mediated ALS.

MATERIALS AND METHODS

Cytochrome C release from isolated mitochondria

Mouse spinal cords and lysates of HEK293T cells (with or without Bcl-2, ATCC cat. # CRL-11268) were homogenized in 800 μl of Buffer A (250 mM Sucrose, 20 mM Hepes-KOH pH 7.5, 10 mM KCl, 1.5 mM $MgCl_2$, 1 mM EDTA, 1 mM EGTA, 1 mM DTT, protease inhibitor) and spun at 750 *g* at 4°C for

10 min. The pellet was re-homogenized in 400 μl of buffer A, spun at 750 *g* at 4°C for an additional 10 min. The supernatants from these two homogenization steps were combined in one solution which was spun twice at 750 *g* at 4°C for 10 min and once at 10 000 *g* at 4°C for 15 min. Each pellet was re-suspended in 80 μl of Buffer B (70 mM Sucrose, 190 mM Mannitol, 20 mM Hepes, pH 7.5 with protease inhibitor). Twenty-five microliters of mitochondria were incubated at room temperature for 30 min with either 1 mM of $CaCl_2$ (Ca Cl_2) or 1 mM of recombinant SOD1 (G93A or A4V oligomers, kindly provided by Drs Andrew Choi and Peter Lansbury, Harvard Medical School) in 20 μl of Buffer B. Twenty-five microliters of untreated (CTL) mitochondria were incubated with 20 μl of Buffer B. Samples were then spun at 100 000 *g* for 1 h at 4°C. The resulting supernatant was then analyzed for Cytochrome C with ELISA following the manufacturer's instruction (R&D Systems, Minneapolis, MN), whereas the resulting mitopellet was re-suspended in Buffer B and analyzed by WB.

Mitopellet for WB analysis of Cytochrome C release was obtained as follows: Petri dishes (10 cm ϕ) were transfected with 700 ng of SOD1 and 700 ng of Bcl-2 using Lipofectamine 2000 following the manufacturer's instructions. After 24 h, cells were detached, washed with 1 ml of PBS, pelletted at 500 rpm and lysed in 100 μl of digitonin extraction buffer (0.025% digitonin, 250 mM sucrose, 10 mM KCl, 1.5 mM $MgCl_2$, 1 mM EDTA, 1 mM EGTA, 20 mM HEPES at pH 7.5) supplemented with complete protease inhibitor (Roche). Lysates were then spun at 15 000 rpm and the resulting pellet containing mitochondria was lysed in 100 μl of RIPA buffer and 20 μg of proteins were loaded onto 15% polyacrylamide gels. WB was then performed using antibodies against Cytochrome C (Cell Signaling, Danvers, MA, USA) or Bcl-2 (BD, San Jose, CA).

Immunofluorescence analysis of mitochondrial integrity

HEK293T cells were plated in two-chamber slides (Lab-Tek) and transfected the following day with 200 ng of SOD1s-eGFP or eGFP alone and 200 ng of Bcl-2 or pcDNA3 alone using Lipofectamine2000 (Invitrogen, Carlsbad, CA, USA) following the manufacturer's instructions. Immunolabeling was performed by fixing the cells for 20 min with a solution of 2% paraformaldehyde/2% sucrose, 10 min with ice-cold methanol, one wash in PBS and 1 h blocking in PBS/5% FBS (Blocking Buffer, BB). Slides were then incubated with primary rabbit antibody anti-Bcl-2 (1:200, Millipore, Billerica, MA, USA), fluorescent-conjugated mouse anti-Cytochrome C (25 μl/well, Alexa Fluor 546, Invitrogen) and secondary anti-rabbit Alexa Fluor 405 (1:200, Invitrogen) for 1 h in BB and rinsed three times in PBS. Cells were then mounted in a solution of 60% glycerol, dried for 2 h, nailpolished and analyzed by confocal microscopy.

Electron microscopy of mitochondrial morphology

Samples were fixed in 2% gluteraldehyde with 1% tannic acid buffered in phosphate buffer (pH 7.4) for o/n at 5°C, rinsed in the same buffer and then exposed to 2% osmium teteraoxide. Following a rinse with double distilled water, samples were put in 0.5% uranyl acetate and then dehydrated in graded steps of acetone (one wash at 25%, 50%, 75%, 95% and three washes at 100%). Samples were then infiltrated with Spurrs resin and polymerized in a 65°C convection oven. The blocks were thin sectioned (70nm) with a Diatome diamond knife on a Leica UCT ultramicrotome, sections analyzed in a FEI Tecnai 12T Electron Microscope and images were digitally recorded with an AMT XR111 camera.

Generation of Bcl-2(AAA)

Generation of Bcl-2(AAA) harboring the triple mutation GDD-AAA at position 101–103 was obtained by amplifying the template plasmid pcDNA3/Bcl-2 with primers F 5′-CCGCCAAGCCGCCGCCGCCTTCTCCCGCC-3′ and R 5′-GGCGGGAGAAGGCGGCGGCGGCTTGGCGG-3′ using Stratagene QuikChange Lightning kit following the manufacturer's instructions (La Jolla, CA, USA).

Immunoprecipitation

SH-SY5Y cells (ATCC cat. # CRL-2266), mouse and human spinal cords were lysed/homogenized in Chaps Buffer (1% CHAPS, 14.5 mM KCl, 5 mM $MgCl_2$, 1 mM EGTA, 1 mM EDTA, 20 mM Tris–HCl pH 7.5) with protease inhibitors (Complete TM, Roche) Samples were pre-cleared for 4 h at 4°C with Biomag magnetic beads (New England Biolabs, Ipswich, MA) and then incubated with anti-Bcl-2 antibodies (α-Bcl-2 Calbiochem, Gibbstown, NJ, α-BH3 Abgent, San Diego, CA and α-pocket BD Pharmingen, San Jose, CA) overnight at 4°C. The antibody–antigen complex was then precipitated with the beads for 4 h at 4°C and precipitates were analyzed by WB using α-Bcl-2 (BD Pharmingen and Santa Cruz, CA). For co-immunoprecipitation, HEK293T cells were lysed in RIPA buffer and 500 μg of lysates were pre-cleared for 4 h at 4°C with magnetic beads (New England Biolabs, Ipswich, MA) and then incubated with the anti-SOD1 antibody (α-SOD1, Santa Cruz, CA) overnight. The antibody–antigen complex was then precipitated with magnetic beads for 4 h at 4°C and precipitates were analyzed by WB using α-Bcl-2 (BD Pharmingen).

Cell viability assay

HEK293T cells were plated into 96 well plates and transfected with either SOD1-eGFP (G93A) alone or in combination with Bcl-2 as described above. Twenty-four hours after transfection, cell viability was scored using the CellTiter-Glo Luminescence Viability Assay (Promega, USA) following the manufacturer's instructions.

SUPPLEMENTARY MATERIAL

Supplementary Material is available at *HMG* online.

ACKNOWLEDGEMENTS

We thank Drs Andy Choi and Peter Lansbury for the generous gift of the recombinant SOD1 proteins.

Conflict of Interest statement. None declared.

FUNDING

This work was supported by the National Institutes of Health [RO1-NS051488 to P.P., RO1-NS064488 to D.T.], the ALS Association [1061 to P.P.] and the Farber Family Foundation. Funding to pay the Open Access Charge was provided by the Farber Family Foundation.

REFERENCES

1. Pasinelli, P. and Brown, R.H. (2006) Molecular biology of amyotrophic lateral sclerosis: insights from genetics. *Nat. Rev. Neurosci.*, **7**, 710–723.
2. Rosen, D.R., Siddique, T., Patterson, D., Figlewicz, D.A., Sapp, P., Hentati, A., Donaldson, D., Goto, J., O'Regan, J.P., Deng, H.X. *et al.* (1993) Mutations in Cu/Zn superoxide dismutase gene are associated with familial amyotrophic lateral sclerosis. *Nature*, **362**, 59–62.
3. Higgins, C.M., Jung, C., Ding, H. and Xu, Z. (2002) Mutant Cu, Zn superoxide dismutase that causes motoneuron degeneration is present in mitochondria in the CNS. *J. Neurosci.*, **22**, RC215.
4. Jaarsma, D., Rognoni, F., van Duijn, W., Verspaget, H.W., Haasdijk, E.D. and Holstege, J.C. (2001) CuZn superoxide dismutase (SOD1) accumulates in vacuolated mitochondria in transgenic mice expressing amyotrophic lateral sclerosis-linked SOD1 mutations. *Acta Neuropathol.*, **102**, 293–305.
5. Liu, J., Lillo, C., Jonsson, P.A., Vande Velde, C., Ward, C.M., Miller, T.M., Subramaniam, J.R., Rothstein, J.D., Marklund, S., Andersen, P.M. *et al.* (2004) Toxicity of familial ALS-linked SOD1 mutants from selective recruitment to spinal mitochondria. *Neuron*, **43**, 5–17.
6. Okado-Matsumoto, A. and Fridovich, I. (2001) Subcellular distribution of superoxide dismutases (SOD) in rat liver: Cu,Zn-SOD in mitochondria. *J. Biol. Chem.*, **276**, 38388–38393.
7. Pasinelli, P., Belford, M.E., Lennon, N., Bacskai, B.J., Hyman, B.T., Trotti, D. and Brown, R.H. Jr (2004) Amyotrophic lateral sclerosis-associated SOD1 mutant proteins bind and aggregate with Bcl-2 in spinal cord mitochondria. *Neuron*, **43**, 19–30.
8. Vande Velde, C., Miller, T.M., Cashman, N.R. and Cleveland, D.W. (2008) Selective association of misfolded ALS-linked mutant SOD1 with the cytoplasmic face of mitochondria. *Proc. Natl. Acad. Sci. USA*, **105**, 4022–4027.
9. Cozzolino, M., Ferri, A. and Carri, M.T. (2008) Amyotrophic lateral sclerosis: from current developments in the laboratory to clinical implications. *Antioxid. Redox Signal*, **10**, 405–443.
10. Wong, P.C., Pardo, C.A., Borchelt, D.R., Lee, M.K., Copeland, N.G., Jenkins, N.A., Sisodia, S.S., Cleveland, D.W. and Price, D.L. (1995) An adverse property of a familial ALS-linked SOD1 mutation causes motor neuron disease characterized by vacuolar degeneration of mitochondria. *Neuron*, **14**, 1105–1116.
11. Kong, J. and Xu, Z. (1998) Massive mitochondrial degeneration in motor neurons triggers the onset of amyotrophic lateral sclerosis in mice expressing a mutant SOD1. *J. Neurosci.*, **18**, 3241–3250.
12. Manfredi, G. and Xu, Z. (2005) Mitochondrial dysfunction and its role in motor neuron degeneration in ALS. *Mitochondrion*, **5**, 77–87.
13. Jung, C., Higgins, C.M. and Xu, Z. (2002) A quantitative histochemical assay for activities of mitochondrial electron transport chain complexes in mouse spinal cord sections. *J. Neurosci. Methods*, **114**, 165–172.
14. Mattiazzi, M., D'Aurelio, M., Gajewski, C.D., Martushova, K., Kiaei, M., Beal, M.F. and Manfredi, G. (2002) Mutated human SOD1 causes dysfunction of oxidative phosphorylation in mitochondria of transgenic mice. *J. Biol. Chem.*, **277**, 29626–29633.
15. Kirkinezos, I.G., Bacman, S.R., Hernandez, D., Oca-Cossio, J., Arias, L.J., Perez-Pinzon, M.A., Bradley, W.G. and Moraes, C.T. (2005) Cytochrome c association with the inner mitochondrial membrane is impaired in the CNS of G93A-SOD1 mice. *J. Neurosci.*, **25**, 164–172.
16. Damiano, M., Starkov, A.A., Petri, S., Kipiani, K., Kiaei, M., Mattiazzi, M., Flint Beal, M. and Manfredi, G. (2006) Neural mitochondrial Ca2+ capacity impairment precedes the onset of motor symptoms in G93A Cu/Zn-superoxide dismutase mutant mice. *J. Neurochem.*, **96**, 1349–1361.
17. Magrane, J. and Manfredi, G. (2009) Mitochondrial function, morphology, and axonal transport in amyotrophic lateral sclerosis. *Antioxid. Redox Signal*, **11**, 1615–1626.
18. Sotelo-Silveira, J.R., Lepanto, P., Elizondo, M.V., Horjales, S., Palacios, F., Martinez Palma, L., Marin, M., Beckman, J.S. and Barbeito, L. (2009) Axonal mitochondrial clusters containing mutant SOD1 in transgenic models of ALS. *Antioxid. Redox Signal*, **11**, 1535–1545.
19. Galluzzi, L., Blomgren, K. and Kroemer, G. (2009) Mitochondrial membrane permeabilization in neuronal injury. *Nat. Rev. Neurosci.*, **10**, 481–494.
20. Gupta, S., Kass, G.E., Szegezdi, E. and Joseph, B. (2009) The mitochondrial death pathway: a promising therapeutic target in diseases. *J. Cell. Mol. Med.*, **13**, 1004–1033.
21. Jourdain, A. and Martinou, J.C. (2009) Mitochondrial outer-membrane permeabilization and remodelling in apoptosis. *Int. J. Biochem. Cell. Biol.*, **41**, 1884–1889.
22. Moll, U.M., Marchenko, N. and Zhang, X.K. (2006) p53 and Nur77/TR3-transcription factors that directly target mitochondria for cell death induction. *Oncogene*, **25**, 4725–4743.
23. Kolluri, S.K., Zhu, X., Zhou, X., Lin, B., Chen, Y., Sun, K., Tian, X., Town, J., Cao, X., Lin, F. *et al.* (2008) A short Nur77-derived peptide converts Bcl-2 from a protector to a killer. *Cancer Cell*, **14**, 285–298.
24. Lin, B., Kolluri, S.K., Lin, F., Liu, W., Han, Y.H., Cao, X., Dawson, M.I., Reed, J.C. and Zhang, X.K. (2004) Conversion of Bcl-2 from protector to killer by interaction with nuclear orphan receptor Nur77/TR3. *Cell*, **116**, 527–540.
25. Chipuk, J.E., Kuwana, T., Bouchier-Hayes, L., Droin, N.M., Newmeyer, D.D., Schuler, M. and Green, D.R. (2004) Direct activation of Bax by p53 mediates mitochondrial membrane permeabilization and apoptosis. *Science*, **303**, 1010–1014.
26. Lei, X., Chen, Y., Du, G., Yu, W., Wang, X., Qu, H., Xia, B., He, H., Mao, J., Zong, W. *et al.* (2006) Gossypol induces Bax/Bak-independent activation of apoptosis and Cytochrome C release via a conformational change in Bcl-2. *FASEB J.*, **20**, 2147–2149.
27. Ray, S.S., Nowak, R.J., Strokovich, K., Brown, R.H. Jr, Walz, T. and Lansbury, P.T. Jr (2004) An intersubunit disulfide bond prevents in vitro aggregation of a superoxide dismutase-1 mutant linked to familial amytrophic lateral sclerosis. *Biochemistry*, **43**, 4899–4905.
28. Gould, T.W., Buss, R.R., Vinsant, S., Prevette, D., Sun, W., Knudson, C.M., Milligan, C.E. and Oppenheim, R.W. (2006) Complete dissociation of motor neuron death from motor dysfunction by Bax deletion in a mouse model of ALS. *J. Neurosci.*, **26**, 8774–8786.
29. Cheng, E.H., Kirsch, D.G., Clem, R.J., Ravi, R., Kastan, M.B., Bedi, A., Ueno, K. and Hardwick, J.M. (1997) Conversion of Bcl-2 to a Bax-like death effector by caspases. *Science*, **278**, 1966–1968.
30. Soo, K.Y., Atkin, J.D., Horne, M.K. and Nagley, P. (2009) Recruitment of mitochondria into apoptotic signaling correlates with the presence of inclusions formed by amyotrophic lateral sclerosis-associated SOD1 mutations. *J. Neurochem.*, **108**, 578–590.
31. Higgins, C.M., Jung, C. and Xu, Z. (2003) ALS-associated mutant SOD1G93A causes mitochondrial vacuolation by expansion of the intermembrane space and by involvement of SOD1 aggregation and peroxisomes. *BMC Neurosci.*, **4**, 16.
32. Kawamata, H., Magrane, J., Kunst, C., King, M.P. and Manfredi, G. (2008) Lysyl-tRNA synthetase is a target for mutant SOD1 toxicity in mitochondria. *J. Biol. Chem.*, **283**, 28321–28328.
33. Schendel, S.L., Xie, Z., Montal, M.O., Matsuyama, S., Montal, M. and Reed, J.C. (1997) Channel formation by antiapoptotic protein Bcl-2. *Proc. Natl. Acad. Sci. USA*, **94**, 5113–5118.
34. Kroemer, G., Galluzzi, L. and Brenner, C. (2007) Mitochondrial membrane permeabilization in cell death. *Physiol. Rev.*, **87**, 99–163.
35. Susnow, N., Zeng, L., Margineantu, D. and Hockenbery, D.M. (2009) Bcl-2 family proteins as regulators of oxidative stress. *Semin. Cancer Biol.*, **19**, 42–49.
36. Grandgirard, D., Studer, E., Monney, L., Belser, T., Fellay, I., Borner, C. and Michel, M.R. (1998) Alphaviruses induce apoptosis in Bcl-2-overexpressing cells: evidence for a caspase-mediated, proteolytic inactivation of Bcl-2. *EMBO J.*, **17**, 1268–1278.
37. Blagosklonny, M.V. (2001) Unwinding the loop of Bcl-2 phosphorylation. *Leukemia*, **15**, 869–874.
38. Zimmermann, A.K., Loucks, F.A., Schroeder, E.K., Bouchard, R.J., Tyler, K.L. and Linseman, D.A. (2007) Glutathione binding to the Bcl-2

homology-3 domain groove: a molecular basis for Bcl-2 antioxidant function at mitochondria. *J. Biol. Chem.*, **282**, 29296–29304.
39. Schlesinger, P.H., Gross, A., Yin, X.M., Yamamoto, K., Saito, M., Waksman, G. and Korsmeyer, S.J. (1997) Comparison of the ion channel characteristics of proapoptotic BAX and antiapoptotic BCL-2. *Proc. Natl. Acad. Sci. USA*, **94**, 11357–11362.
40. Nguyen, K.T., Garcia-Chacon, L.E., Barrett, J.N., Barrett, E.F. and David, G. (2009) The Psi(m) depolarization that accompanies mitochondrial Ca2+ uptake is greater in mutant SOD1 than in wild-type mouse motor terminals. *Proc. Natl. Acad. Sci. USA*, **106**, 2007–2011.
41. Reed, J.C., Zha, H., Aime-Sempe, C., Takayama, S. and Wang, H.G. (1996) Structure-function analysis of Bcl-2 family proteins. Regulators of programmed cell death. *Adv. Exp. Med. Biol.*, **406**, 99–112.
42. Jonas, E.A. (2009) Molecular participants in mitochondrial cell death channel formation during neuronal ischemia. *Exp. Neurol.*, **218**, 203–212.
43. Bruijn, L.I., Miller, T.M. and Cleveland, D.W. (2004) Unraveling the mechanisms involved in motor neuron degeneration in ALS. *Annu. Rev. Neurosci.*, **27**, 723–749.
44. Pasinelli, P., Borchelt, D.R., Houseweart, M.K., Cleveland, D.W. and Brown, R.H. Jr (1998) Caspase-1 is activated in neural cells and tissue with amyotrophic lateral sclerosis-associated mutations in copper-zinc superoxide dismutase. *Proc. Natl. Acad. Sci. USA*, **95**, 15763–15768.
45. Pasinelli, P., Houseweart, M.K., Brown, R.H. Jr and Cleveland, D.W. (2000) Caspase-1 and -3 are sequentially activated in motor neuron death in Cu,Zn superoxide dismutase-mediated familial amyotrophic lateral sclerosis. *Proc. Natl. Acad. Sci. USA*, **97**, 13901–13906.
46. Vukosavic, S., Stefanis, L., Jackson-Lewis, V., Guegan, C., Romero, N., Chen, C., Dubois-Dauphin, M. and Przedborski, S. (2000) Delaying caspase activation by Bcl-2: a clue to disease retardation in a transgenic mouse model of amyotrophic lateral sclerosis. *J. Neurosci.*, **20**, 9119–9125.
47. Kostic, V., Jackson-Lewis, V., de Bilbao, F., Dubois-Dauphin, M. and Przedborski, S. (1997) Bcl-2: prolonging life in a transgenic mouse model of familial amyotrophic lateral sclerosis. *Science*, **277**, 559–562.